Geoderma 448 (2024) 116936

Contents lists available at ScienceDirect

Geoderma

journal homepage: www.elsevier.com/locate/geoderma

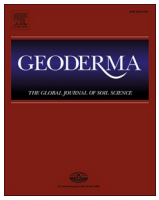

Newly plant-derived carbon in the deeper vadose zone of a sandy agricultural soil does not stimulate denitrification

Wenyi Xu [a,b,*], Per Lennart Ambus [b]

[a] Department of Soil and Environment, Swedish University of Agricultural Sciences, Lennart Hjelms väg 9, Uppsala, Sweden
[b] Department of Geosciences and Natural Resource Management, University of Copenhagen, Denmark

ARTICLE INFO

Handling Editor: C. Rumpel

Keywords:
Bulk soil carbon
Hot- and cold-water extractable carbon
Incubation experiment
Respired CO_2-C
Denitrification enzyme activity
$\delta^{13}C$ signature
Ultraviolet visible spectral analyse

ABSTRACT

Analysis of stable carbon (C) isotopic signatures ($\delta^{13}C$) in various soil C pools provides useful information on soil C sources, transport, and availability. Understanding the extent of deeper soil (below 40 cm) sequestration and transport of plant derived C is of particular interest as this provides a source for microorganisms to drive biological denitrification (as indicated by denitrification enzyme activity, DEA) and hence mitigate the nitrate leaching to groundwater. Meanwhile, studies on deeper soil C sequestration are rare due to methodological constraints. This study was done in deeper vadose zone (0–160 cm) of a sandy agricultural soil in a humid and temperature zone after a C_3-C_4 vegetation change taking advantage of the marked isotopic differences between C_3 and C_4 plants. It took place in a site previously grown with C_3 crops (beet, barley, grass), but where C_4 crops (maize) were grown continuously for the last 20 years. The other site where C_3 crops were continuously grown was used for comparison. Specifically, the $\delta^{13}C$ signature in top and deeper soil layers was used to distinguish between old C_3– and newly C_4-plant derived C in four C pools, i.e., bulk soil C, hot- and cold-water extractable C, and respired CO_2-C. The $\delta^{13}C$ signature between C_3 soils and C_3-C_4 shifted soils was similar for bulk soil C but significantly different for water extractable and respired C pools. Hence, we estimated that the contribution of newly derived C to bulk soil C was negligible, whereas the contributions to the other C pools amounted up to 28.4 % along the soil profile. This emphasizes the importance of simultaneously analysing $\delta^{13}C$ signature in various soil C pools to accurately assess C vertical transport and distribution. The concentrations of cold-DOC and values of specific ultraviolet visible absorbance of the wavelengths 254 and 280 nm decreased from 50 to 130 cm soil depths, while they increased below these depths. However, this suggested rise in C chemical quality at the deepest soil depths did not cause an increase in soil respiration activity or DEA, which was attributed to the protective effects of iron and aluminium oxides on C decomposition. Upon the application of labile C and N substrates, the deepest soil layers displayed a significantly increased DEA, suggesting the presence of a relatively abundant population of active denitrifying organisms. Overall, this study documents the presence of plant-derived C in the deeper vadose zone. Meanwhile, this particular C pool might not be an important substrate to drive deep-soil denitrification due to constraints imposed by the protection by metal oxides.

1. Introduction

The excessive use of chemical nitrogen (N) fertilizers in intensive agricultural areas worldwide has resulted in significant environmental issues, including nitrate (NO_3^-) leaching, ammonia volatilization, and greenhouse gas emissions (Hakeem et al., 2017; Dimkpa et al., 2020; Puga et al., 2020). Nitrate leaching resulting from agricultural practices has been shown to accumulate in the subsurface soil, known as the vadose zone (Ascott et al., 2016; Liu et al., 2022). In the deep vadose zone, biological denitrification is widely recognized as a beneficial process for reducing leached NO_3^- (Xin et al., 2019). However, the availability of soil organic carbon (C) is often considered as the major limiting factor for denitrification in the vadose zone (Peterson et al., 2013; Chen et al., 2018). Furthermore, the C availability controls the rate of carbon dioxide (CO_2) flux to the atmosphere, affects microbial activity and composition, and reflects C sequestration capacity (Singh et al., 2009; Schimel and Schaeffer, 2012).

Soil organic C (SOC) consists of various heterogeneous pools that differ in their stability and availability (Pausch and Kuzyakov, 2012; Novara et al., 2013). New C pools are more decomposable by

* Corresponding author.
E-mail address: wenyi.xu@slu.se (W. Xu).

https://doi.org/10.1016/j.geoderma.2024.116936
Received 8 November 2023; Received in revised form 29 March 2024; Accepted 5 June 2024
Available online 22 June 2024

microorganisms compared with old, recalcitrant C pools (Lützow et al., 2006; Novara et al., 2014). To distinguish between new and old C pools and to determine their contributions to SOC, isotopic tracer techniques have been used. Due to a distinct isotopic composition of C_3 and C_4 plants, a vegetation conversion from C_3 to C_4 plants can lead to a different isotopic composition of new and old C pools, which allows for their separation (Balesdent and Mariotti, 1996; Flessa et al., 2000; Werth and Kuzyakov, 2008). Generally it is observed that contents of SOC and newly C_4 plant-derived C (upon C_3-C_4 plant transition) decrease with increasing soil depth due to the decreasing root biomass and associated root exudates (Kramer and Gleixner, 2008; Müller et al., 2016; Liu et al., 2019). For example, Liu et al. (2019) found that the proportion of newly-derived C varied from 46 % to 5 % as soil depth increased from 0 to 100 cm after a 30-year continuous C_4-plant cultivation (changing from C_3-plant) in an Ultisol. However, in the deep vadose zone (below 100 cm), a long residence time of water and low oxygen (O_2) concentrations (that decrease with depth) could generally constrain microbial decomposition of organic C (Peterson et al., 2013). In addition, the accumulation of iron (Fe) and aluminium (Al) oxides in deep soil layers probably result in the stabilization of soil organic compounds, thus reducing microbiological activity and mineralization rates (Rumpel and Kögel-Knabner, 2010; Wu et al., 2020). Therefore, the vertical patterns of SOC and the contributions of new and old C pools in the deeper vadose zone are likely to differ from those in the overlying soil layers.

Dissolved organic C (DOC), a relatively small and partially labile C pool, can serve as readily available substrates for soil microorganisms or become stable components of SOM through adsorption onto mineral surfaces (Bolan et al., 2011; Ramesh et al., 2019). Previous studies have shown a rapid decline in soil DOC concentrations with increasing depth down to 100 cm (Vinther et al., 2006; Don and Schulze, 2008). However, there is a scarcity of information regarding the bioavailability of DOC, especially in the deeper vadose zone (below 100 cm), despite the recognition that the quality of DOC is vital in regulating denitrification of leached NO_3^- in subsoils (Peterson et al., 2013).

Soil microbial respiration is controlled by the quantity and quality of soil C pools (e.g., labile and recalcitrant C) and environmental conditions (e.g., temperature, soil moisture and redox conditions). Microbial respiration predominantly takes place in the topsoil, with respiration rates diminishing markedly as soil depth increases (Fang and Moncrieff, 2005). Comparing the contributions of new and old C to respired CO_2 allows for a quantitative estimation of the availability of C in relation to the time it is entering the soil (Flessa et al., 2000; Pausch and Kuzyakov, 2012).

Many studies examine the changes in $\delta^{13}C$ signature along with soil profile following a shift from C_3 to C_4 plants based on bulk soil C or SOC pools (Kristiansen et al., 2005; Rasse et al., 2006; Schneckenberger and Kuzyakov, 2007; Christensen et al., 2011). However, the preferential utilization of new versus old C and the cascade of C decomposition processes cause variations in the magnitude of $\delta^{13}C$ increase (caused by change to C_4 plant) between soil C pools (Flessa et al., 2000; Blagodatskaya et al., 2011; Pausch and Kuzyakov, 2012). For example, Blagodatskaya et al. (2011) found that the $\delta^{13}C$ increase was higher in microbial biomass (>13 ‰) than that in SOC (8.3 ‰), respired CO_2-C (6.2 ‰) and DOC pools (4.7 ‰) in top soil (0–10 cm) 12 years after C_3-C_4 vegetation change. Therefore, to gain a comprehensive understanding of the vertical distribution of newly derived C and the lability of C within the soil profile, further investigations are needed to assess the changes in $\delta^{13}C$ signature across various C pools and the depth-wise contributions of newly derived C to these C pools.

Information on the quantity and lability of C in vadose zones of agricultural soils is essential for a thorough assessment of the inherent capability of soils to protect groundwater from NO_3^- contamination (Soana et al., 2022). The objective of this study is to assess the characteristics of soil C in the vadose zone in a Danish agricultural field positioned in a humid and temperate climatic zone. The study has a particular emphasis to investigate i) the vertical distribution of the newly plant-derived C, and ii) the bioavailability of C in the deeper vadose zone. In order to answer these compelling questions, we analysed the changes in stable ^{13}C-isotopic characteristics in bulk soil C, water soluble C and respired CO_2, along the soil profile 20 years following a C_3-C_4 transition. Additionally, we assessed the chemical quality of soluble C by ultraviolet–visible (UV–Vis) spectral analyses and the potential of this particular C pool to provide a substrate for biological denitrification via a denitrification enzyme activity assay. We hypothesize that: (I) the vertical distribution of the newly plant-derived C in deep soil depths cannot be accurately accessed via changes in ^{13}C signature in bulk soil C due to the limited amount of newly plant-derived C, but is better understood by examining water-extractable and respired C pools due to its preferential utilization; and (II) the concentrations of DOC and its chemically labile fractions increase in the deepest soil depths (below 130 cm) due to decreasing oxygen availability and thus suppressed C decomposition, which serves as an important C substrate to drive denitrification.

2. Methodology

2.1. Site description

The study site is located in a field where agriculture practices have been ongoing since 1860, within a periglacial terrain near the town St. Darum in Southwestern Jutland, Denmark (55°24′36′′N, 8°42′45′′E). The soil has developed in meltwater sand of Weichselian age (about 12000 yr BP) in a humid (mean annual precipitation 808 mm) and temperate climate (mean annual temperature of 9.3 °C) (Cappelen, 2021). The site was selected to represent a C_3– to C_4-shift in dominant vegetation, and hence to trace the fate of C_4 plant sequestered carbon. The current field has been cropped with maize (*Zea mays*) in monoculture, for fodder purposes, over the past 20 years. Maize represents the C_4-photosynthetic physiology, and typically has a carbon $^{13}C/^{12}C$ isotopic signature ($\delta^{13}C$) of −13.39 ‰ (Kristiansen et al., 2004; Christensen et al., 2011). Prior to this time frame, the field was cropped only with C_3 plants typical for this region such as barley (*Hordeum vulgare*), wheat (*Triticum aestivum*) and fodder beat (*Beta vulgaris*) exhibiting a $\delta^{13}C$ of ca. −29.0 ‰ (Basu et al., 2015). In order to have a basis for comparison of the isotopic imprint of C_4 plants on SOC isotopic characteristics, reference sites with C_3 plants only but under comparable management regimes, climate and soil characteristics, are required. No fields in the immediate adjacency met this requirement with a documented long-term history of C_3 cropping only, as maize is often included in local crop rotations. Consequently, we included three different C_3 fields from other parts of the peninsula of Jutland. One site is located in Rostrup (55°44′47′′N, 9°17′26′′E) in the Middle Eastern Jutland, and two sites are located in Humlum (56°31′43′′N, 8°33′28′′E) and Vildbjerg (56°9′32′′N, 8°46′33′′E), respectively, in the Middle Western Jutland, all within less than 60 km radius from the C_3-C_4 site. The locations of the reference sites are under similar climatic conditions to avoid differences in isotopic fractionation due to drought-related stress. It is assumed that baseline soil organic matter qualities among the sites is similar. Throughout this study, referring to the C_3 reference sites is thus a calculated average of the characteristics between these three sites, and C_4-plant derived C (accumulated over the last 20 years) is referred to as newly derived C.

2.2. Soil sampling and analysis

In June 2018, triplicate soil core samples from the vadose zone (7 cm Ø; 0–160 cm below surface) were collected at three positions separated by 8–40 m in the Darum site (C_3-C_4 site). Similarly, soil core samples were collected in duplicate or triplicate (separated by 25–100 m) at each of the Rostrup, Vildbjerg, and Humlum sites (C_3 reference sites). The soil cores were stored refrigerated (5 °C) in horizontal position constrained in the sampling liners (Eijkelkamp, Giesbeek, NL). For analyses, the soil was gently removed from the liner at the specific depths and coarse roots

and stones removed by hand.

Soil pH was measured in a 1:2.5 soil:liquid slurry with 10 mM calcium chloride ($CaCl_2$). Iron (Fe) and aluminium (Al) contents were extracted using citrate-bicarbonate-dithionite (CBD) (Mehra and Jackson, 1960) and measured on an ICP-MS (Elan 6100DRC, Perkin-Elmer) with a multi-element scanning method (TotalQuantTM119, Perkin-Elmer). The quantity and quality of the extracted organic C are influenced by the temperature used during extraction (Jones and Willett, 2006). Cold- and hot-water extractable organic C was obtained by a sequential procedure. First step in the procedure was a cold-water extraction (20 C) with field moist soil in milli-Q water (1:5) that was carefully mixed on a horizontal shaker (200 rpm) for 1 h. After centrifugation at 3000 g for 20 min, the supernatant was filtered at 0.45 μm (Q-max syringe filter (cellulose acetate), Frisenette Aps, Ebeltoft, Denmark) and stored at 5 ℃ until analysis. Second step, for the hot-water extraction (70 ℃), the soil in the centrifuge tube was resuspended in milli-Q water (1:5) and kept in water bath for 1 h during which the slurry was hand-shaken regularly. After centrifugation at 3000 g, the supernatant was treated as described for the cold-water extraction. The cold- and hot-water extractable organic C throughout the text is referred to as cold and hot dissolved organic C (cold-DOC and hot-DOC), respectively. The cold-DOC originates from the recently decomposed soil C or from animal excreta and soluble plant residues. The hot-DOC is a component of the labile C and also closely related to soil microbial biomass and micro aggregation (Ghani et al., 2003). Two different labile C fractions are analyzed as supplementary indicators of soil C quality. Cold- and hot-water extractable C was measured at a Total Organic Carbon Analyzer (TOC-V_{CPH}, Shimadzu, Tokyo, Japan). Nitrate (NO_3^-) in cold water extracts was measured using a Metrohm Anion system (Metrohm, Herisau, Switzerland). The filtered cold-water extracts were transferred to quarts cuvettes (Suprasil, Hellma, Jena, Germany) prior to 120 to 700 nm scanning, using a UV-1800 Spectrophotometer (Shimadzu, Tokyo, Japan). The ultraviolet–visible absorbance spectra analysis of cold-DOC can provide insights into the composition, stability, and reactivity of DOC. It reveals the presence of aromatic compounds, degree of humification, molecular size distribution, photodegradation potential, and the source and origin of organic matter (Li and Hur, 2017). The UV- spectra analysis was done only for the samples from the C_3-C_4 site (Fig. S1), due to the results assumed to be similar among the C_3 and C_3-C_4 sites. Twenty-five millilitres of filtered extracts were subsequently freeze-dried and encapsulated into tins for $^{13}C/^{12}C$-ratio analysis. Subsamples of the oven-dried soil (70 ℃) were homogenized in an agate ball mill, and the finely ground material were transferred to tin foil capsules (10 mg for topsoil samples and 20 mg for subsoil samples). Total C, N and $\delta^{13}C$ of the bulk soil and freeze-dried material were analyzed by isotopic ratio mass spectrometry (IRMS) using a Thermo Delta V Advantage IRMS (Thermo Scientific, Bremen, Germany) coupled in continuous flow mode to an elemental analyser (Flash 2000, Thermo Scientific, Bremen, Germany). As working standard for IRMS analyses, we used pure CO_2 gas calibrated against certified ^{13}C-sucrose (IAEA, Vienna, Austria).

2.3. Soil incubation

To assess the bioavailability of SOC, we determined soil respiratory activity and the $\delta^{13}C$ value of respired CO_2. Field moist subsamples (10 g) were weighed into 100 mL infusion bottles that were closed airtight with butyl septa. Headspace gas was sampled at 0, 24, 48, 72 and 144 h and transferred to evacuated 3-mL Exetainers (Labco Scientific, High Wycombe, UK). The gas samples were analyzed for their CO_2 concentrations and the corresponding $\delta^{13}C$ signature on a Thermo Delta V Advantage IRMS coupled in continuous flow mode to a GasBench II (Thermo Scientific).

Denitrification enzyme activity (DEA) bioassay was deployed with three different substrate combinations, i.e. control (no N or C), KNO_3 only (N) and KNO_3 + C (NC). The DEA was done only for the samples from the C_3-C_4 site (Fig. S1), due to the results assumed to be similar among the C_3 and C_3-C_4 sites. Ten-g portions of field-moist soil was weighed into 100-mL infusion bottles and added with 15-mL (1:1.5 w:v) pure milli-Q water, 1 mM KNO_3, or combination of 1 mM KNO_3, 0.5 mM glucose ($C_6H_{12}O_6$), 0.5 mM sodium acetate ($C_2H_3NaO_2$) and 0.5 mM monosodium succinate ($C_4H_5NaO_4$). After substrate addition, the infusion flasks were sealed and three times repeatedly evacuated and pressurized with di-nitrogen (N_2) gas in order to obtain anaerobic conditions, and 10-mL of acetylene injected into the headspace to inhibition the last step of the denitrification from N_2O to N_2 (Xu et al., 2021). The bottles were shaken vigorously by hand and left at room temperature for subsequent sampling of the headspace N_2O using same procedure as describe above. Headspace sampling was carried out at 0, 6, 12, 24, 36, 48, 60 and 72 h, and the gas samples were analyzed for their N_2O concentrations by gas chromatography on a HP7890 Agilent equipped with Electron Capture Detector (Agilent Technologies, Santa Clara, USA).

2.4. Calculations and statistics

The results of the respiration incubations were processed using the Keeling plot procedure to encounter the $\delta^{13}C$ of respired CO_2. This is expressed by the Y-axis intercept of the best fit linear regression line between the headspace $\delta^{13}C$-CO_2 on the inverse of the CO_2 concentration (Keeling, 1958). A reduced major axis regression as proposed by Pataki et al. (2003) was used (Model II) to take into account a coupled variance on the horizontal and vertical axes. Outliers in the Keeling analysis were removed from the data set. All reported results had $R^2 > 0.80$.

The proportion of maize-derived C (C_4) in the bulk soil C, hot- and cold-water extractable C, and respired CO_2 pools was calculated according to the equation:

$$f(\%) = \frac{\delta^{13}C_t - \delta^{13}C_{reference}}{\delta^{13}C_{maize} - \delta^{13}C_{reference}} \times 100$$

where $\delta^{13}C_t$ is the $\delta^{13}C$ value of the C pool under C_3-C_4 vegetation change, and $\delta^{13}C_{reference}$ and $\delta^{13}C_{maize}$ are the $\delta^{13}C$ values of the corresponding C pool in reference soil with continuous C_3 vegetation and in pure maize residues, respectively. $\delta^{13}C_{maize}$ was calculated as an average of values reported in the literature (Collins et al., 2000; Kristiansen et al., 2004; Christensen et al., 2011).

The specific ultraviolet absorbance of the wavelengths 254 nm (SUVA-254) and 280 nm (SUVA-280) was calculated by the equation:

$$\frac{Au_{\lambda nm} \bullet 100}{conc_{DOC}}$$

where $Au_{\lambda\ nm}$ is absorbance of the specific wavelength and $conc_{DOC}$ is the concentrations of cold-water extractable organic C.

Prior to statistical analysis, we inspected the QQ-plots and used Shapiro-Wilk normality test or Levene's test to check data for normal distribution and homogeneity of variance, and data were log or square root transformed when necessary. We tested depth differences in bulk soil C and N, C:N ratio, cold-DOC, hot-DOC and soil microbial respiration, by using one-way ANOVA model. The effects of C_3-C_4 vegetation change and soil depth on $\delta^{13}C$ values of the C pools, and the effects of substrate addition and soil depth on the DEA, were assessed by two-way ANOVA model. Post hoc pairwise comparisons between levels of the significant factor were then conducted using the emmeans package, with Tukey's Honestly Significant Differences (Tukey HSD) *p*-value adjustment (Lenth, 2020). The significant differences or effects are based on $p \leq 0.05$. Pearson correlation analysis was performed to explore the correlations between soil chemical properties, soil microbial respiration, SUVA-250 and SUVA-280 values from the C_3-C_4 site. All analysis above was performed using R software v. 3.6.1 (Team, 2019).

3. Results

3.1. Soil chemical properties

Soil chemical properties of the C_3-C_4 site profile are shown in Table 1. The bulk soil C concentrations decreased with depth to approximately 85 cm, and remained constant until 130 cm depth, below which a small increase was observed (Table 1). The bulk N concentrations were almost constantly low throughout the profile (Table 1). The C:N ratio of the topsoil layer was the lowest with a value of 13, and the subsoil layers (70–100 and 90–100 cm) showed significantly higher C:N ratios ranging from 57 to 97 (Table 1).

The DOC concentrations of the cold- and hot-water extractions showed similar concentrations throughout the profile. In accordance with bulk soil C concentrations, the cold- and hot-DOC concentrations decreased with soil depth to 85 cm, and generally remained constant until 130 cm depth ($p < 0.01$; Table 1). Below 130 depth the cold-DOC concentrations increased with depth from 12.6 to 27.9 mg kg^{-1} ($p < 0.01$), while the hot-DOC concentration significantly increased to 15.5 mg kg^{-1} at 130–140 cm depth ($p < 0.01$) and remained constant to 160 cm depth (Table 1).

The pattern for the NO_3^- concentrations also showed the highest values in the topsoil, decreasing concentrations below and overall increasing values below 120 cm depth (Table 1).

The pH values of the site were moderately acidic. The plough layer had a pH value of 5.66 seemingly preserved by management practices (Table 1). Beneath the topsoil layer the pH ranged between 4.63 and 4.92, except for a noticeable decrease down to 2.53 in the 85–100 cm depth interval (Table 1).

The Al and Fe concentrations in the CBD extractions were the highest in the topsoil (1323 and 944 mg kg^{-1}, respectively; Table 1). Decreasing concentrations were then seen throughout the profile, with the exception of the deepest sample intervals (130–160 cm) where Al and Fe concentrations were seemingly increasing (Table 1).

3.2. Stable C isotopes

Due to the uncertainty in $\delta^{13}C$ analysis arising from low bulk soil C concentrations in deep soil depths (>80 cm), bulk soil $\delta^{13}C$ values were only reported in soil depths down to 80 cm (Fig. S2 and Table S2). The C_3-C_4 site exhibited consistent bulk soil $\delta^{13}C$ values across different depths, with $\delta^{13}C$ varying between −29 ‰ and −27 ‰ (Fig. S2). Moreover, the bulk soil C in the C_3-C_4 site was isotopically indistinguishable from the reference site (Fig. S2).

In accordance with the bulk soil C concentrations, the topsoil layers (0–30 cm) showed significantly higher respiratory activity than subsoil layers ($p < 0.01$; Fig. 1). The $\delta^{13}C$ values of respired CO_2 had a significant isotopic difference between the C_3-C_4 and reference sites ($p < 0.01$; Fig. S3). At the C_3-C_4 site, the $\delta^{13}C$ in CO_2 averaged –26.3 ‰, 4.2 delta units less negative than the reference site throughout the entire soil profile (Fig. S3).

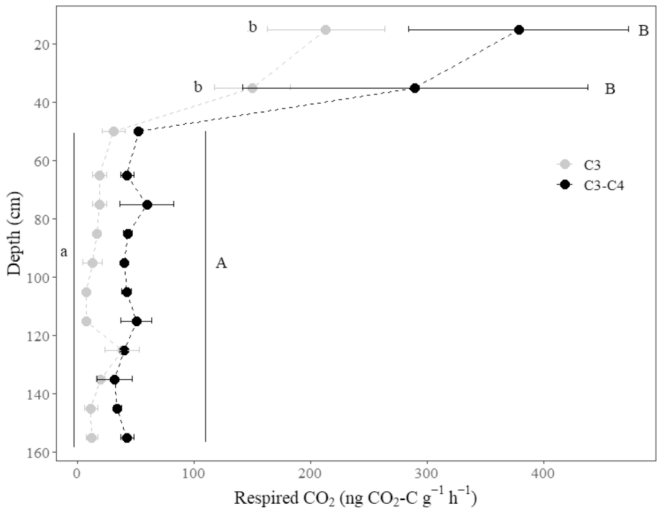

Fig. 1. Soil respiration activity along with soil depth at the C_3 and C_3-C_4 sites. Error bars are standard error. Lowercase and uppercase letters indicate significant differences between soil depth intervals ($p < 0.05$) at the C_3 and C_3-C_4 sites, respectively.

The proportions of maize-derived C in the cold-DOC, hot-DOC, and respired CO_2-C pools are shown in Fig. 2. The bulk soil C pool only showed minor influence from maize in the topsoil (0.8 %) and no maize-derived C was evident in the subsoil layers (Fig. 2). The cold-DOC and hot-DOC pools also had high proportions of maize-derived C at the topsoil (0–40 cm), and at 40–120 cm depths a decline was observed for the hot-DOC pool (Fig. 2). Below 120 cm, a relatively high amount of maize-derived C was present in the cold-DOC and hot-DOC pools (Fig. 2). The respired CO_2-C pool was highly influenced by maize-derived C, and on average 23 % of respired CO_2-C across different depths was inherited from maize-derived C (Fig. 2).

3.3. Denitrification enzyme activity

The non-amended soils showed the highest N_2O production rates in the topsoil layer and negligible denitrification activity below 40 cm depth (Fig. 3).

As was the case for the non-amended soils, the greatest N_2O production activity was detected in the topsoil layer, but the NO_3^- addition

Table 1
Soil chemical properties along with soil depth at the C_3-C_4 site.

Depth (cm)	Total C (%)	Total N (%)	C:N	Cold-DOC (mg kg^{-1})	Hot-DOC (mg kg^{-1})	NO_3^--N (mg kg^{-1})	pH	Al (mg kg^{-1})	Fe (mg kg^{-1})
0–30	3.29 ± 0.44^{c}	0.26 ± 0.04^{b}	13 ± 0^{a}	37.4 ± 1.0^{e}	69.8 ± 0.5^{g}	172.37	5.66	1322	934
40–60	0.29 ± 0.00^{b}	0.01 ± 0.00^{a}	24 ± 0^{ab}	39.9 ± 1.0^{e}	39.2 ± 0.4^{f}	2.61	4.74	856	530
60–70	0.22 ± 0.02^{ab}	0.01 ± 0.00^{a}	28 ± 7^{ab}	30.4 ± 0.9^{d}	33.9 ± 0.4^{e}	0.58	4.77	549	461
70–80	0.18 ± 0.05^{ab}	$<0.01^{a}$	82 ± 21^{c}	21.1 ± 0.9^{c}	20.8 ± 0.4^{d}	1.39	4.74	477	427
80–85	0.07 ± 0.00^{a}	<0.01a	97 ± 0^{c}	10.2 ± 0.8^{ab}	11.4 ± 0.4^{a}	1.33	4.66	405	365
85–90	0.06 ± 0.00^{a}	<0.01a	40 ± 0^{abc}	10.7 ± 0.8^{ab}	12.7 ± 0.4^{b}	3.62	2.53	349	279
90–100	0.06 ± 0.02^{a}	$<0.01^{a}$	57 ± 19^{bc}	10.3 ± 0.8^{ab}	11.4 ± 0.4^{ab}	1.93	3.72	371	267
100–110	0.05 ± 0.02^{a}	$<0.01^{a}$	29 ± 10^{ab}	10.9 ± 0.8^{ab}	9.9 ± 0.4^{a}	1.96	4.63	317	248
110–120	0.06 ± 0.00^{a}	$<0.01^{a}$	40 ± 0^{abc}	13.4 ± 0.9^{b}	11.4 ± 0.4^{ab}	1.64	4.85	301	295
120–130	0.05 ± 0.00^{a}	$<0.01^{a}$	33 ± 0^{ab}	9.0 ± 0.9^{a}	9.8 ± 0.4^{a}	2.11	4.88	272	218
130–140	0.09 ± 0.00^{ab}	$<0.01^{a}$	56 ± 0^{abc}	12.6 ± 0.9^{ab}	15.5 ± 0.4^{c}	7.06	4.90	340	185
140–150	0.13 ± 0.00^{a}	$<0.01^{a}$	38 ± 10^{abc}	17.1 ± 1.0^{c}	16.3 ± 0.5^{c}	4.53	4.92	401	216
150–160	0.19 ± 0.00^{a}	0.01 ± 0.00^{a}	31 ± 9^{a}	27.9 ± 1.1^{d}	16.9 ± 0.5^{c}	8.01	4.83	486	243

Hot-water extractable C (hot-DOC) and cold-water extractable C (cold-DOC). Concentrations of citrate-bicarbonate-dithionite (CBD) extractable Al and Fe. Numbers show means (±standard error) of replicates (n = 3), except for soil NO_3^--N, pH, Al and Fe concentrations (n = 1). Lowercase letters indicate significant differences between soil depth intervals ($p < 0.05$).

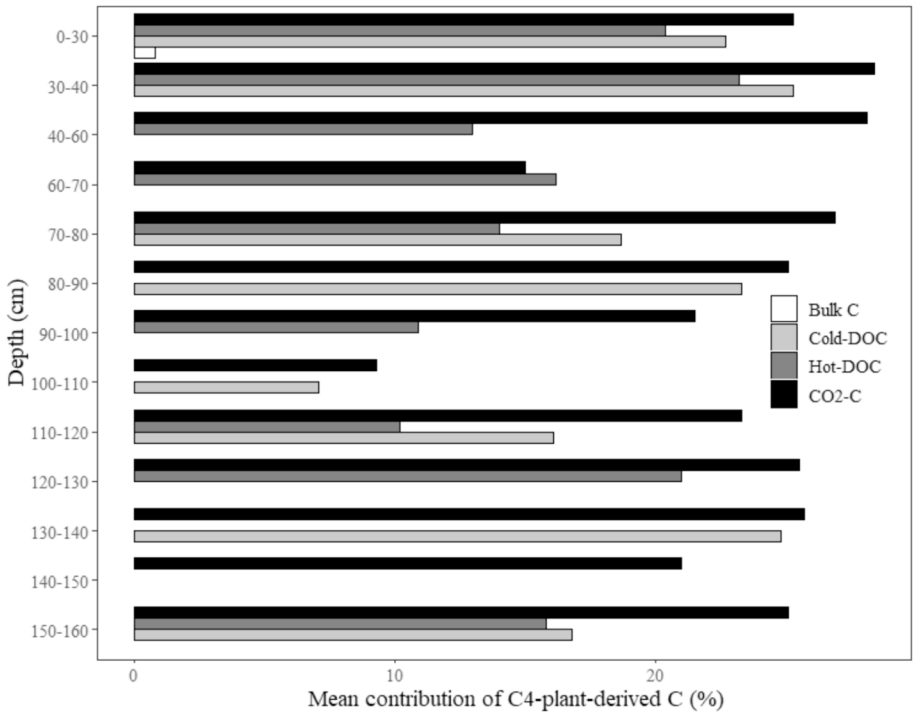

Fig. 2. Mean contribution of C_4-plant-derived C to bulk soil C, cold-water and hot-water extractable C, and respired CO_2.

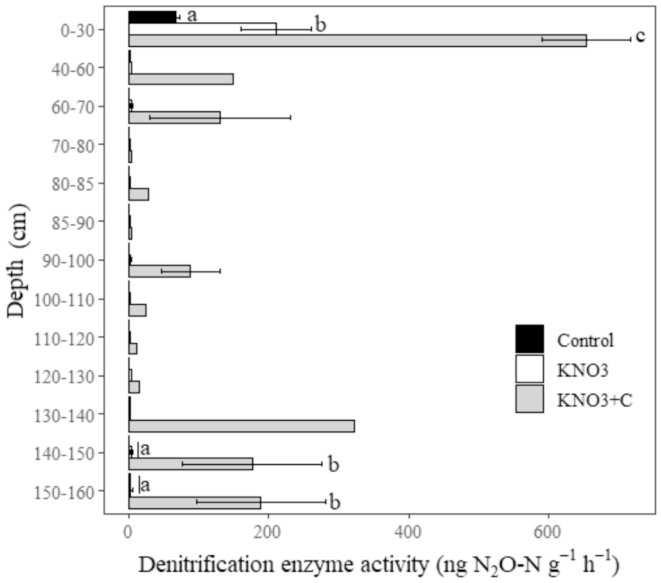

Fig. 3. Denitrification enzyme activity in response to three substrate additions along with soil depth at the C_3-C_4 site. Substrate additions: control, KNO_3 addition, and KNO_3 + glucose-C addition. Error bars are standard error. Lowercase letters indicate significant differences between three substrate addition treatments at each soil depth interval ($p < 0.05$).

caused a threefold increase in the activity compared to the non-amended treatment ($p < 0.01$; Fig. 3). The subsoil samples with NO_3^- addition also systematically showed small N_2O activity throughout the depths of the profile, and the activity with NO_3^- addition did not significantly differ from the non-amended treatment (Fig. 3).

The N_2O activity after combined NO_3– and C- substrate addition at the topsoil layer was significantly higher than that of the deeper soil layers ($p < 0.05$; Fig. 3). The topsoil layer displayed a ten-fold increase of N_2O activity compared to the non-amended treatment, and an activity three times the size of the NO_3^- treatment ($p < 0.01$; Fig. 3). Moreover, the subsoil depths also responded positively to the additional C amendment, but with diverse patterns through the profile (Fig. 3). The intervals of 40–70 cm and 130–160 cm showed much higher activities than the depth interval of 70–130 cm ($p < 0.01$; Fig. 3). At the deepest soil layers (130–160 cm), the N_2O activity after combined NO_3^- and C substrate addition was significantly higher than the other two treatments ($p < 0.01$; Fig. 3).

3.4. Ultraviolet visible absorbance spectra

The ultraviolet visible absorbance spectra from 190-500 nm wavelength of five selected soil depths from the C_3-C_4 site is shown in Fig. S4. The topsoil layer exhibited the highest absorbance spectrum with a prominent peak between 200–205 nm, and a smaller shoulder between 275 and 300 nm (Fig. S4). The three intermediate soil depths (40–60, 60–70 and 100–110 cm) had reduced absorbance spectra and did not show distinct absorbance peaks, but merely a decreasing pattern in absorbance units with increasing wavelength (Fig. S4). Absorbance intensity of the deepest soil interval (150–160 cm) exceeded that of the superior 100–110 cm soil layer, and a peak was evident around 200 nm, close to that of the topsoil layer (Fig. S4).

The topsoil layer exhibited SUVA-280 and SUVA-254 values of 4.4 and 5.7 L mg^{-1} m^{-1}, respectively (Fig. 4). An increasing trend in SUVA-280 and SUVA-254 values was observed from 40 to 140 cm depths (Fig. 4). The lowermost depth intervals of 130–160 cm showed an abrupt decrease in the index values from 4.9 to 2.9 and from 6.5 to 3.9, respectively (Fig. 4). This resulted in significantly lower values at the deepest depth (150–160 cm) compared with the upper depth intervals (80–150 cm; $p < 0.01$; Fig. 4).

3.5. Correlations between DOC concentrations, and the specific ultraviolet absorbance, metal concentrations and soil respiration

The Pearson correlation analysis showed that soil cold-DOC concentrations across depths were negatively correlated with SUVA-254 (R^2 = -0.76) and SUVA-280 values (R^2 = -0.73; $p < 0.01$; Fig. 5). Soil

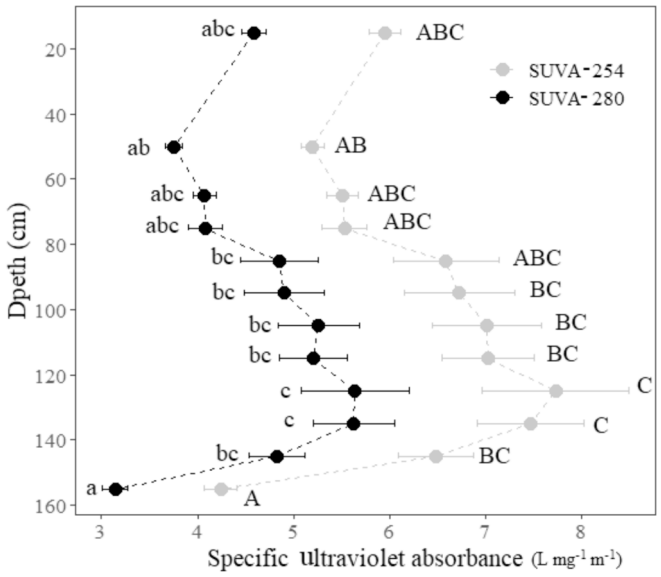

Fig. 4. The specific ultraviolet absorbance of the wavelengths 254 nm (SUVA-254) and 280 nm (SUVA-280) along with soil depth at the C_3-C_4 site. Error bars are standard error. Lowercase letters indicate significant differences in SUVA-280 values between soil depth intervals ($p < 0.05$). Uppercase letters indicate significant differences in SUVA-254 values between soil depth intervals ($p < 0.05$).

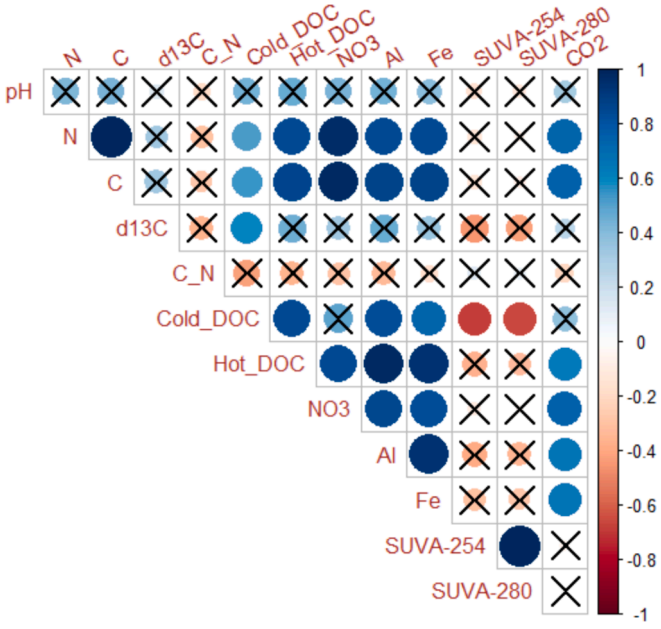

Fig. 5. Pearson correlation analysis between DOC concentrations, and the specific ultraviolet absorbance, metal concentrations and soil respiration. d13C: $\delta^{13}C$ of bulk soil C, Hot_DOC: hot-water extractable C, Cold_DOC: cold-water extractable C, NO3: soil NO_3^--N, SUVA-254 and SUVA-280: the specific ultraviolet absorbance of the wavelengths 254 nm and 280 nm. The colors indicate positive or negative correlations and the size of circles signifies the strength of the correlations. Non-significant correlations ($p > 0.05$) are marked with × .

cold-DOC and hot-DOC concentrations were both positively correlated with soil Al and Fe concentration ($R^2 > 0.55$; $p < 0.01$; Fig. 5).

4. Discussion

4.1. Depth distribution of newly plant-derived C

Our results showed that C_4-plant-derived CO_2-C and DOC pools were present throughout the soil profile down to at least 160 cm depth, supporting hypothesis I that the vertical distribution of the newly plant-derived C in deep soil depths is better understood by examining water-extractable and respired C pools.

Stable ^{13}C-isotope analyses have been carried out to quantify the contribution of newly plant derived C to the bulk soil C pools with notably emphasis on deeper soil C sequestration and availability. Here, and throughout we use the term "newly" to indicate the C sequestered over the last 20 years of C_4 cropping. Since C_3 plants have a more negative $\delta^{13}C$ signature than C_4 plants (Christensen et al., 2011), C_3-C_4 shift in crops can cause an increase in $\delta^{13}C$ of soil C pools, at least in the topsoil layer (Thomsen and Christensen, 2010). However, the $\delta^{13}C$ signal in bulk soil C from the study site (with 20 years of continuous C_4 cropping) did not show any difference from the reference sites (only with C_3 cropping). This is likely because the deposition of C_4-C is too little to change bulk soil ^{13}C pool.

A significant difference was observed between the $\delta^{13}C$ signals of respired CO_2. Here, the C_3–C_4 study site showed less negative isotopic signatures than the reference site with a difference of up to 4.5 ‰ $\delta^{13}C$ values. The rather larger uncertainty of the signals from the study site compared to the reference signals is likely caused by the newly introduced maize and is therefore reflecting heterogeneity of the input of C_4-plant-derived C into a soil previously with a sole C_3 plant isotopic imprint. According to the proportions of maize-derived CO_2-C and DOC, small pools of C_4-plant-derived C were present throughout the soil profile down to at least 160 cm depth. This indicates that the newly plant C is a limited yet pervasive constituent of the soil C pool and is available to microbial oxidation to support respiratory activity. The higher contribution of recent C to CO_2-C (9.3–27.9 %) and DOC (6.3–25.4 %) compared with that to the bulk soil C pool (≤0.8 %), indicates that organic C originated from C_4-C was preferably decomposed compared to old C with C_3 signature. This is consistent with the observations by Blagodatskaya et al. (2011) that after a C_3-C_4 vegetation change, the preferential utilization of the recent versus the old C was the primary driver for the changes of $\delta^{13}C$ values in soil pools. Pausch and Kuzyakov (2012) also demonstrated that the organics recently introduced into the soil (C_4-C) were more easily available for microorganisms compared with C previously stabilized in soil (C_3-C). Further, microorganisms throughout the soil, even several meters below the soil surface, have been reported to metabolize organic C that is substantially younger than the soil organic C (Scheibe et al., 2023). Therefore, the preferential microbial utilization of C_4-C may explain the lack of difference in bulk soil $\delta^{13}C$ signal observed between the study and reference sites. Within the rooting zone, the C_4-plant imprint on the C isotopic signature is caused by the presence of maize roots as well as root exudates (Schrumpf et al., 2013). At lower depths, the maize-derived C can be transported either by bioturbation or more likely in the form of soluble C (e.g., DOC) (Bailey et al., 2019). This is supported by the fact that the C_4-plant-derived DOC exhibited a distribution throughout the soil profile down to at least 160 cm depth.

Although soil CO_2 efflux rates and the overall quantity of recently C_4-plant-derived CO_2-C decreased markedly from topsoil (0–40 cm) to subsoil (below 40 cm), the contribution of recent C to CO_2 generally remained consistent across soil depths. The decreased soil respiration activities were linked to the decreased bulk soil C and hot-DOC concentrations (Fig. 5), which can be attributed to factors such as declining root biomass, root exudates, soil C quality, and variations in microbial community composition between top and deeper soil layers (Stone et al.,

2014; Shahid et al., 2017; Tückmantel et al., 2017; Li et al., 2021). The contribution of recently plant-derived C to SOC has been reported to decrease with increasing soil depth due to decreasing recent C input (Kramer and Gleixner, 2008; Müller et al., 2016; Liu et al., 2019). Liu et al. (2019) found that in an Ultisol after a C_3-C_4 crop transition, the proportion of maize-derived C decreased from 31-46 % of soil organic C in top 0–20 cm depth to 5 % at 100 cm depth. Kramer and Gleixner (2008) reported that newly plant-derived C constituted 12 % and 3 % of SOC at 0–20 cm and 40–60 cm depths, respectively, after 40-year maize cultivation in a Haplic Phaeozem. In the current study, the contribution of recently plant-derived C was only detected in the topsoil, but it was found to be negligible (0.8 % of bulk soil C). Despite utilizing the same crop cover (maize), the contrasting proportions of maize-derived C in SOC are likely due to differences in soil types, cultivation duration, soil management practices, and climate conditions. The consistent contribution of recently plant-derived CO_2-C across soil depths suggests a relatively uniform proportion of C_4-plant-derived labile C along the soil profile, considering respired CO_2 as an indicator of labile SOC (Benbi et al., 2015; Li et al., 2019). This is supported by the comparable contribution of C_4-plant-derived DOC at deeper soil layers (e.g., 15.8–24.8 % at 120–140 cm depths), as found in the topsoil (20.4–22.7 %; Fig. 2).

4.2. Depth distribution of C bioavailability

Our data showed that the concentrations of DOC and its chemically labile fractions increase in the deepest soil depths (below 130 cm), partly supporting our hypothesis II.

The concentrations of bulk soil C and N, cold- and hot water extracted DOC and NO_3^--N, were at maximum in the topsoil layer (0–30 cm) and showed relatively high concentrations in the uppermost 40–80 cm of the soil profile. Relatively high concentrations were also seen in the depth intervals of 130–160 cm, which is somewhat surprising as these parameters usually decrease steadily with soil depth (Ghani et al., 2010; Xiaosong et al., 2023). The lowermost samples were collected just above the groundwater table, and therefore it can be speculated that the increasing concentrations of these soil parameters in the deepest subsoil are partially owed to the decreasing oxygen availability and thus suppressed decomposition rates of SOC. Moreover, interaction with the mineral phase, in particular amorphous Fe and Al oxides, can lead to protection of SOC from microbial decomposition in subsoil horizons of acidic soils (Das et al., 2019; Gartzia-Bengoetxea et al., 2020). This protective mechanism is supported by the fact that increasing cold-DOC concentration was paralleled by increasing concentrations of CBD extractable Fe and Al in the deepest depth intervals. According to chemical analysis with pyrolysis-field ionization mass spectrometry, the hot-water extractable C contained more carbohydrates, phenols, lignin monomers and displayed greater biodegradability than the cold-water extractable C (Landgraf et al., 2006; Bankó et al., 2021; Wang et al., 2021). Thus, the notably higher topsoil hot-DOC concentrations suggests a substantial amount of readily degradable soluble C in this layer, which originates from root exudates and low molecular compounds derived from litter (Müller et al., 2009; Baumert et al., 2018). This explains the significantly lower soil respiration activity in subsoil depths where hot-DOC concentrations have markedly declined. Generally, SOM in deep soil layers is older and more decomposed, and thus soil C:N ratios are typically decreasing with soil depth (Rumpel and Kögel-Knabner, 2010; Guillaume et al., 2015). The relatively high C:N ratios observed in the 70–140 cm depth intervals were due to very low bulk soil N concentrations, which reached the analytical detection limit in some depth intervals.

Throughout the soil profile, soil was moderately acidic to acidic, especially at the depth intervals of 85–100 cm where soil pH was ≤ 3.72. It is well-known that the long-term application of N fertilizers can cause significant pH reductions in topsoil and even downward acidification in the soil profile (Fontoura et al., 2019; Xu et al., 2023). This is particularly the case for our sandy soils that have low pH buffering capacity. Vertical transport of soil water with a high solute concentration due to excess of N fertilizers not only explain the low pH values, but also the relatively high NO_3^- concentrations in the 85–100 cm intervals. The highly acidic soil in these depths suggests that the subsoil is more vulnerable to acidification caused by N fertilization. A previous study also reported that strong soil acidification extended to a depth of 150–200 cm in sandy farmlands in the western part of Jutland, Demark (Balstrøm et al., 2013). In our study area, many soils have also shown frequent occurrence of iron sulfides, which can undergo oxidation to produce iron oxides and sulphuric acid and cause extremely low soil pH (Madsen et al., 1985).

Despite a large amount of C in topsoil, the DEA increased after the N addition, to a lower extent compared with the N + C addition. In subsoil layers, no apparent response of the DEA was observed to the N addition. This suggests limited availability of existing soil C to denitrifying microorganisms within the deeper soil profile. Our results are in accordance with the observations by Chen et al. (2018) who documented comparable vertical patterns of denitrification rates along soil profile in a vadose zone under grain cropping and suggested the severe scarcity of labile C in deep soil horizons. In contrast to the intermediate soil layers (40–130 cm), the lowermost depth intervals (130–160 cm) exhibited particularly high DEA when combined N and C substrates were applied. This suggests the presence of a relatively high abundance of active denitrifying organisms in the deepest soil layers, probably because increasing DOC concentrations alleviate C limitation to some extent. The C availability has been shown to play a crucial role in determining the vertical distribution of denitrifier abundance in agricultural soils (Peterson et al., 2013; Loeppmann et al., 2016; Chen et al., 2018).

The SUVA-254 and SUVA-280 have been reported to be positively correlated with the degree of aromaticity and molecular weight (Peacock et al., 2014; Rodríguez et al., 2016). In the current study, the two UV–Vis parameters decreased gradually from 40 to 130 cm soil depths, and then a marked increase was observed at the lowermost depths. This suggests a decreasing level of aromatic DOC structures and increasing contribution of small organic molecules to cold-DOC in the deepest soil depths, and thus provides additional supports for increased C availability in these deepest layers. Meanwhile, the low respiratory activity in the deepest depth intervals (130–160 cm) contradicts the implication drawn from the increasing cold-DOC concentrations and SUVA characteristics. Typically cold-DOC has been reported to be less available than readily available substrates such as glucose and hot-DOC (Blagodatskaya et al., 2011; Gunina and Kuzyakov, 2015), and the respiratory activity in C-poor environment is probably relatively insensitive to the changes in cold-DOC concentrations and is expected to remain at a low level. This is confirmed by a strong relationship between soil respiration and hot-DOC rather than cold-DOC. In addition, soil respiration is limited in deeper soil depths because the energy content of the soil organic matter declines with increasing soil depth (Ni et al., 2020). Soil respiration at the bottom of the soil profile can also be constrained due to the stabilizing effects of Fe and Al oxides on organic C (Das et al., 2019; Gartzia-Bengoetxea et al., 2020).

5. Conclusions

This study addresses the knowledge gap of the vertical distribution of newly plant-derived C and the bioavailability of C in the deeper vadose zone under sandy agricultural soil. It was carried out in a field subject to C_3-C_4 crop transition over the past 20 years, and soil C sequestration and vertical distribution was determined from a combination of stable ^{13}C-isotopic composition in various soil C-pools, chemical analyses, and bioassays. The contribution of newly derived C to bulk soil C was negligible, but its contributions to water soluble C and respired CO_2 were pronounced (up to 28.4 %) throughout the soil profile. The increasing C concentrations and chemical quality in the deepest soil depths did not result in increasing soil respiration activity or DEA, which

was attributed to the protection of C by Fe and Al oxides. When labile C and N substrates were applied, the deepest soil depths exhibited noticeably high DEA, suggesting the presence of a relatively high abundance of active denitrifying organisms. The study emphasizes the importance of simultaneous analysis of the $\delta^{13}C$ signature of various soil C pools for the estimation of vertical distribution of newly derived C and its bioavailability and potential for respiratory activities. However, the increasing chemical lability of C in the deeper vadose zone may not act as a driving force for denitrification to mitigate NO_3^- leaching, primarily due to increased protection by metal oxides.

CRediT authorship contribution statement

Wenyi Xu: Data curation, Formal analysis, Visualization, Writing – original draft, Writing – review & editing. **Per Lennart Ambus:** Conceptualization, Funding acquisition, Investigation, Methodology, Project administration, Supervision, Writing – review & editing.

Declaration of competing interest

The authors declare that they have no known competing financial interests or personal relationships that could have appeared to influence the work reported in this paper.

Data availability

Data will be made available on request.

Acknowledgements

We are grateful to the late Senior scientist Vibeke Ernstsen at the Geological Survey of Denmark and Greenland (GEUS) and late Professor Henrik Breuning-Madsen at the Department of Geosciences and Natural Resource Management (IGN) for their inspiring work to initiating, designing and accomplishing current work. We would like to thank Anne Christine Krull Pedersen (IGN) who coordinated and executed much of the field- and lab work, Christina Rosenberg Lynge (GEUS) for lab assistance, and Senior scientist Christian Nyrop Albers (GEUS) for methodological discussions. Henrik Germundsson at the Ytteborg Field Trials company helped identifying experimental sites. The study received financial support from Geocenter Denmark and Land-CRAFT, the Pioneer Center for Research in Sustainable Agricultural Futures (DNRF grant P2).

Appendix A. Supplementary data

Supplementary data to this article can be found online at https://doi.org/10.1016/j.geoderma.2024.116936.

References

Ascott, M., Wang, L., Stuart, M., Ward, R., Hart, A., 2016. Quantification of nitrate storage in the vadose (unsaturated) zone: a missing component of terrestrial N budgets. Hydrol. Process. 30, 1903–1915.
Bailey, V.L., Pries, C.H., Lajtha, K., 2019. What do we know about soil carbon destabilization? Environ. Res. Lett. 14, 083004.
Balesdent, J., Mariotti, A., 1996. Measurement of soil organic matter turnover using 13C natural abundance. Mass Spectrom. Soil. 83–111.
Balstrøm, T., Breuning-Madsen, H., Krüger, J., Jensen, N.H., Greve, M.H., 2013. A statistically based mapping of the influence of geology and land use on soil pH: A case study from Denmark. Geoderma 192, 453–462.
Bankó, L., Tóth, G., Marton, C.L., Hoffmann, S., 2021. Hot-water extractable C and N as indicators for 4p1000 goals in a temperate-climate long-term field experiment: A case study from Hungary. Ecol. Ind. 126, 107364.
Basu, S., Agrawal, S., Sanyal, P., Mahato, P., Kumar, S., Sarkar, A., 2015. Carbon isotopic ratios of modern C3–C4 plants from the Gangetic Plain, India and its implications to paleovegetational reconstruction. Palaeogeogr. Palaeoclimatol. Palaeoecol. 440, 22–32.
Baumert, V.L., Vasilyeva, N.A., Vladimirov, A.A., Meier, I.C., Kögel-Knabner, I., Mueller, C.W., 2018. Root exudates induce soil macroaggregation facilitated by fungi in subsoil. Front. Environ. Sci. 6, 140.
Benbi, D.K., Brar, K., Toor, A.S., Singh, P., 2015. Total and labile pools of soil organic carbon in cultivated and undisturbed soils in northern India. Geoderma 237, 149–158.
Blagodatskaya, E., Yuyukina, T., Blagodatsky, S., Kuzyakov, Y., 2011. Turnover of soil organic matter and of microbial biomass under C3–C4 vegetation change: Consideration of 13C fractionation and preferential substrate utilization. Soil Biol. Biochem. 43, 159–166.
Bolan, N.S., Adriano, D.C., Kunhikrishnan, A., James, T., McDowell, R., Senesi, N., 2011. Dissolved organic matter: biogeochemistry, dynamics, and environmental significance in soils. Adv. Agron. 110, 1–75.
Cappelen, J., 2021. World Weather Records 1991–2020. DMI Report 21.
Chen, S., Wang, F., Zhang, Y., Qin, S., Wei, S., Wang, S., Hu, C., Liu, B., 2018. Organic carbon availability limiting microbial denitrification in the deep vadose zone. Environ. Microbiol. 20, 980–992.
Christensen, B.T., Olesen, J.E., Hansen, E.M., Thomsen, I.K., 2011. Annual variation in δ13C values of maize and wheat: Effect on estimates of decadal scale soil carbon turnover. Soil Biol. Biochem. 43, 1961–1967.
Collins, H., Elliott, E., Paustian, K., Bundy, L., Dick, W., Huggins, D., Smucker, A., Paul, E., 2000. Soil carbon pools and fluxes in long-term corn belt agroecosystems. Soil Biol. Biochem. 32, 157–168.
Das, R., Purakayastha, T., Das, D., Ahmed, N., Kumar, R., Biswas, S., Walia, S., Singh, R., Shukla, V., Yadava, M., 2019. Long-term fertilization and manuring with different organics alter stability of carbon in colloidal organo-mineral fraction in soils of varying clay mineralogy. Sci. Total Environ. 684, 682–693.
Dimkpa, C.O., Fugice, J., Singh, U., Lewis, T.D., 2020. Development of fertilizers for enhanced nitrogen use efficiency–Trends and perspectives. Sci. Total Environ. 731, 139113.
Don, A., Schulze, E.-D., 2008. Controls on fluxes and export of dissolved organic carbon in grasslands with contrasting soil types. Biogeochemistry 91, 117–131.
Fang, C., Moncrieff, J.B., 2005. The variation of soil microbial respiration with depth in relation to soil carbon composition. Plant and Soil 268, 243–253.
Flessa, H., Ludwig, B., Heil, B., Merbach, W., 2000. The origin of soil organic C, dissolved organic C and respiration in a long-term maize experiment in Halle, Germany, determined by 13C natural abundance. J. Plant Nutr. Soil Sci. 163, 157–163.
Fontoura, S.M.V., de Castro Pias, O.H., Tiecher, T., Cherubin, M.R., de Moraes, R.P., Bayer, C., 2019. Effect of gypsum rates and lime with different reactivity on soil acidity and crop grain yields in a subtropical Oxisol under no-tillage. Soil Tillage Res. 193, 27–41.
Gartzia-Bengoetxea, N., Virto, I., Arias-González, A., Enrique, A., Fernández-Ugalde, O., Barré, P., 2020. Mineral control of organic carbon storage in acid temperate forest soils in the Basque Country. Geoderma 358, 113998.
Ghani, A., Dexter, M., Perrott, K., 2003. Hot-water extractable carbon in soils: a sensitive measurement for determining impacts of fertilisation, grazing and cultivation. Soil Biol. Biochem. 35, 1231–1243.
Ghani, A., Müller, K., Dodd, M., Mackay, A., 2010. Dissolved organic matter leaching in some contrasting New Zealand pasture soils. Eur. J. Soil Sci. 61, 525–538.
Guillaume, T., Damris, M., Kuzyakov, Y., 2015. Losses of soil carbon by converting tropical forest to plantations: erosion and decomposition estimated by delta(13) C. Glob. Chang. Biol. 21, 3548–3560.
Gunina, A., Kuzyakov, Y., 2015. Sugars in soil and sweets for microorganisms: review of origin, content, composition and fate. Soil Biol. Biochem. 90, 87–100.
Hakeem, K.R., Sabir, M., Ozturk, M., Akhtar, M.S., Ibrahim, F.H., 2017. Nitrate and nitrogen oxides: sources, health effects and their remediation. Rev. Environ. Contam. Toxicol. 242, 183–217.
Jones, D.L., Willett, V.B., 2006. Experimental evaluation of methods to quantify dissolved organic nitrogen (DON) and dissolved organic carbon (DOC) in soil. Soil Biol. Biochem. 38, 991–999.
Keeling, C.D., 1958. The concentration and isotopic abundances of atmospheric carbon dioxide in rural areas. Geochim. Cosmochim. Acta 13, 322–334.
Kramer, C., Gleixner, G., 2008. Soil organic matter in soil depth profiles: distinct carbon preferences of microbial groups during carbon transformation. Soil Biol. Biochem. 40, 425–433.
Kristiansen, S., Brandt, M., Hansen, E., Magid, J., Christensen, B., 2004. 13C signature of CO2 evolved from incubated maize residues and maize-derived sheep faeces. Soil Biol. Biochem. 36, 99–105.
Kristiansen, S., Hansen, E., Jensen, L., Christensen, B., 2005. Natural 13C abundance and carbon storage in Danish soils under continuous silage maize. Eur. J. Agron. 22, 107–117.
Landgraf, D., Leinweber, P., Makeschin, F., 2006. Cold and hot water–extractable organic matter as indicators of litter decomposition in forest soils. J. Plant Nutr. Soil Sci. 169, 76–82.
Lenth, R., 2020. Emmeans: Estimated Marginal Means, aka Least-Squares Means. Rpackage version 1.4. 7. 2020.
Li, P., Hur, J., 2017. Utilization of UV-Vis spectroscopy and related data analyses for dissolved organic matter (DOM) studies: A review. Crit. Rev. Environ. Sci. Technol. 47, 131–154.
Li, J., Li, H., Zhang, Q., Shao, H., Gao, C., Zhang, X., 2019. Effects of fertilization and straw return methods on the soil carbon pool and CO2 emission in a reclaimed mine spoil in Shanxi Province, China. Soil Tillage Res. 195, 104361.
Li, J., Pei, J., Dijkstra, F.A., Nie, M., Pendall, E., 2021. Microbial carbon use efficiency, biomass residence time and temperature sensitivity across ecosystems and soil depths. Soil Biol. Biochem. 154, 108117.

Liu, M., Min, L., Wu, L., Pei, H., Shen, Y., 2022. Evaluating nitrate transport and accumulation in the deep vadose zone of the intensive agricultural region, North China Plain. Sci. Total Environ. 825, 153894.
Liu, S., Zhang, Z.B., Li, D.M., Hallett, P.D., Zhang, G.L., Peng, X.H., 2019. Temporal dynamics and vertical distribution of newly-derived carbon from a C3/C4 conversion in an Ultisol after 30-yr fertilization. Geoderma 337, 1077–1085.
Loeppmann, S., Blagodatskaya, E., Pausch, J., Kuzyakov, Y., 2016. Enzyme properties down the soil profile-A matter of substrate quality in rhizosphere and detritusphere. Soil Biol. Biochem. 103, 274–283.
Lützow, M.v., Kögel-Knabner, I., Ekschmitt, K., Matzner, E., Guggenberger, G., Marschner, B., Flessa, H., 2006. Stabilization of organic matter in temperate soils: mechanisms and their relevance under different soil conditions–a review. Eur. J. Soil Sci. 57, 426–445.
Madsen, H.B., Jensen, N.H., Jakobsen, B.H., Platou, S.W., 1985. A method for identification and mapping potentially acid sulfate soils in Jutland, Denmark. Catena 12, 363–371.
Müller, M., Alewell, C., Hagedorn, F., 2009. Effective retention of litter-derived dissolved organic carbon in organic layers. Soil Biol. Biochem. 41, 1066–1074.
Müller, K., Kramer, S., Haslwimmer, H., Marhan, S., Scheunemann, N., Butenschön, O., Scheu, S., Kandeler, E., 2016. Carbon transfer from maize roots and litter into bacteria and fungi depends on soil depth and time. Soil Biol. Biochem. 93, 79–89.
Ni, X., Liao, S., Tan, S., Peng, Y., Wang, D., Yue, K., Wu, F., Yang, Y., 2020. The vertical distribution and control of microbial necromass carbon in forest soils. Glob. Ecol. Biogeogr. 29, 1829–1839.
Novara, A., Gristina, L., Kuzyakov, Y., Schillaci, C., Laudicina, V., La Mantia, T., 2013. Turnover and availability of soil organic carbon under different M editerranean land-uses as estimated by 13C natural abundance. Eur. J. Soil Sci. 64, 466–475.
Novara, A., La Mantia, T., Rühl, J., Badalucco, L., Kuzyakov, Y., Gristina, L., Laudicina, V.A., 2014. Dynamics of soil organic carbon pools after agricultural abandonment. Geoderma 235, 191–198.
Pataki, D., Ehleringer, J., Flanagan, L., Yakir, D., Bowling, D., Still, C., Buchmann, N., Kaplan, J.O., Berry, J., 2003. The application and interpretation of Keeling plots in terrestrial carbon cycle research. Global Biogeochem. Cycles 17.
Pausch, J., Kuzyakov, Y., 2012. Soil organic carbon decomposition from recently added and older sources estimated by δ13C values of CO2 and organic matter. Soil Biol. Biochem. 55, 40–47.
Peacock, M., Evans, C.D., Fenner, N., Freeman, C., Gough, R., Jones, T.G., Lebron, I., 2014. UV-visible absorbance spectroscopy as a proxy for peatland dissolved organic carbon (DOC) quantity and quality: considerations on wavelength and absorbance degradation. Environ. Sci. Processes Impacts 16, 1445–1461.
Peterson, M., Curtin, D., Thomas, S., Clough, T., Meenken, E., 2013. Denitrification in vadose zone material amended with dissolved organic matter from topsoil and subsoil. Soil Biol. Biochem. 61, 96–104.
Puga, A.P., Grutzmacher, P., Cerri, C.E.P., Ribeirinho, V.S., de Andrade, C.A., 2020. Biochar-based nitrogen fertilizers: greenhouse gas emissions, use efficiency, and maize yield in tropical soils. Sci. Total Environ. 704, 135375.
Ramesh, T., Bolan, N.S., Kirkham, M.B., Wijesekara, H., Kanchikerimath, M., Rao, C.S., Sandeep, S., Rinklebe, J., Ok, Y.S., Choudhury, B.U., 2019. Soil organic carbon dynamics: Impact of land use changes and management practices: A review. Adv. Agron. 156, 1–107.
Rasse, D.P., Mulder, J., Moni, C., Chenu, C., 2006. Carbon turnover kinetics with depth in a French loamy soil. Soil Sci. Soc. Am. J. 70, 2097–2105.
Rodríguez, F.J., Schlenger, P., García-Valverde, M., 2016. Monitoring changes in the structure and properties of humic substances following ozonation using UV–Vis, FTIR and 1H NMR techniques. Sci. Total Environ. 541, 623–637.
Rumpel, C., Kögel-Knabner, I., 2010. Deep soil organic matter—a key but poorly understood component of terrestrial C cycle. Plant Soil 338, 143–158.
Scheibe, A., Sierra, C.A., Spohn, M., 2023. Recently fixed carbon fuels microbial activity several meters below the soil surface. Biogeosciences 20, 827–838.
Schimel, J.P., Schaeffer, S.M., 2012. Microbial control over carbon cycling in soil. Front. Microbiol. 3, 348.
Schneckenberger, K., Kuzyakov, Y., 2007. Carbon sequestration under Miscanthus in sandy and loamy soils estimated by natural 13C abundance. J. Plant Nutr. Soil Sci. 170, 538–542.
Schrumpf, M., Kaiser, K., Guggenberger, G., Persson, T., Kögel-Knabner, I., Schulze, E.-D., 2013. Storage and stability of organic carbon in soils as related to depth, occlusion within aggregates, and attachment to minerals. Biogeosciences 10, 1675–1691.
Shahid, M., Nayak, A.K., Puree, C., Tripathi, R., Lal, B., Gautam, P., Bhattacharyya, P., Mohanty, S., Kumar, A., Panda, B.B., Kumar, U., Shukla, A.K., 2017. Carbon and nitrogen fractions and stocks under 41 years of chemical and organic fertilization in a sub-humid tropical rice soil. Soil Tillage Res. 170, 136–146.
Singh, K., Ghoshal, N., Singh, S., 2009. Soil carbon dioxide flux, carbon sequestration and crop productivity in a tropical dryland agroecosystem: Influence of organic inputs of varying resource quality. Appl. Soil Ecol. 42, 243–253.
Soana, E., Vincenzi, F., Colombani, N., Mastrocicco, M., Fano, E.A., Castaldelli, G., 2022. Soil Denitrification, the Missing Piece in the Puzzle of Nitrogen Budget in Lowland Agricultural Basins. Ecosystems 25, 633–647.
Stone, M., DeForest, J., Plante, A., 2014. Changes in extracellular enzyme activity and microbial community structure with soil depth at the Luquillo Critical Zone Observatory. Soil Biol. Biochem. 75, 237–247.
Team, R.C., 2019. R: A language and environment for statistical computing (Version 3.6. 1)[Software package]. Vienna, Austria: R Foundation for Statistical Computing. Retrieved from.
Tückmantel, T., Leuschner, C., Preusser, S., Kandeler, E., Angst, G., Mueller, C.W., Meier, I.C., 2017. Root exudation patterns in a beech forest: dependence on soil depth, root morphology, and environment. Soil Biol. Biochem. 107, 188–197.
Vinther, F.P., Hansen, E.M., Eriksen, J., 2006. Leaching of soil organic carbon and nitrogen in sandy soils after cultivating grass-clover swards. Biol. Fertil. Soils 43, 12–19.
Wang, Z., Ren, J., Xu, C., Geng, Z., Du, X., Li, Y., 2021. Characteristics of water extractable organic carbon fractions in the soil profiles of Picea asperata and Betula albosinensis forests. J. Soil. Sediment. 21, 3580–3589.
Werth, M., Kuzyakov, Y., 2008. Root-derived carbon in soil respiration and microbial biomass determined by 14C and 13C. Soil Biol. Biochem. 40, 625–637.
Wu, H., Song, X., Liu, F., Zhao, X., Zhang, G.-L., 2020. Regolith property controls on nitrate accumulation in a typical vadose zone in subtropical China. Catena 192, 104589.
Xiaosong, Y., Zhengyi, H., Zijian, X., Songyan, L., Xiaolei, S., Xianlin, K., Mingming, T., 2023. Low soil C: N ratio resulted in the accumulation and leaching of nitrite and nitrate in agricultural soil under heavy rainfall. Pedosphere.
Xin, J., Liu, Y., Chen, F., Duan, Y., Wei, G., Zheng, X., Li, M., 2019. The missing nitrogen pieces: A critical review on the distribution, transformation, and budget of nitrogen in the vadose zone-groundwater system. Water Res. 165, 114977.
Xu, W., Prieme, A., Cooper, E.J., Mörsdorf, M.A., Semenchuk, P., Elberling, B., Grogan, P., Ambus, P.L., 2021. Deepened snow enhances gross nitrogen cycling among Pan-Arctic tundra soils during both winter and summer. Soil Biol. Biochem. 160.
Xu, W., Zhao, D., Ma, Y., Yang, G., Ambus, P.L., Liu, X., Luo, J., 2023. Effects of long-term organic fertilizer substitutions on soil nitrous oxide emissions and nitrogen cycling gene abundance in a greenhouse vegetable field. Appl. Soil Ecol. 188, 104877.